Supplementary Material for:

Meltwater drainage and iceberg calving observed in high spatiotemporal resolution at Helheim Glacier, Greenland

Sierra M. Melton[1], Richard B. Alley[1], Sridhar Anandakrishnan[1], Byron R. Parizek[1,2], Michael G. Shahin[3,4], Leigh A. Stearns[3,4], Adam L. LeWinter[5], David C. Finnegan[5]

[1]Department of Geosciences, and Earth and Environmental Systems Institute, Pennsylvania State University, University Park, PA, USA

[2]Mathematics and Geoscience, Pennsylvania State University, DuBois, PA, USA

[3]Department of Geology, University of Kansas, Lawrence, KS, USA

[4]Center for Remote Sensing of Ice Sheets, University of Kansas, Lawrence, KS, USA

[5]Cold Regions Research and Engineering Laboratory, Hanover, NH, USA

DATA AND METHODS

Satellite imagery

Table S1: Relevant specifications for the satellite imagery used. Note the significant difference in spatial resolution of Maxar imagery (IKONOS, QuickBird, GeoEye-1, and WorldView-1, -2, -3) compared to that of Landsat-8 and Sentinel-2.

Satellite	Years used in this study	Panchromatic resolution (m)	Multispectral resolution (m)
IKONOS	2011-14	0.82	3.2
QuickBird	2011-14	0.55-0.61	2.16-2.44
WorldView-1	2011-19	0.50	N/A
GeoEye-1	2011-19	0.41	1.65
WorldView-2	2011-19	0.46	1.84
WorldView-3	2014-19	0.31	1.24
Landsat-8	2013-19	15	30
Sentinel-2A/B	2015/16-19	N/A	10

Supraglacial meltwater

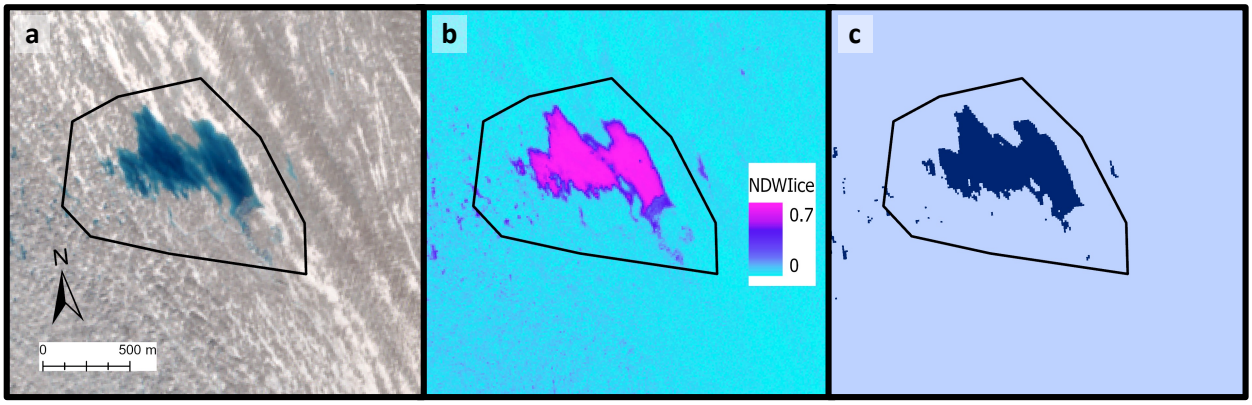

Figure S1: Illustrated representation of the NDWIice classification process for the supraglacial lake L, beginning with (a) true-color Sentinel-2 imagery from 23 July 2017. (b) After completing the NDWIice calculation, higher output values highlight meltwater pooling on the glacier surface. Here high values, corresponding with the lake area in (a), are shown in magenta. (c) Pixels with an NDWIice value above the threshold are classified as water (dark blue). The black outline is the shapefile area used to define the lake. The total area of water pixels within the black outline represents the surface area of the lake.

Tidal phase with calving

We modeled the tidal cycle within Sermilik Fjord with Arc5km2018 (Erofeeva & Egbert, 2020), a barotropic tide model on a 5 km polar stereographic grid. Modeled 2020 tides were consistent with forecasted 2020 tide data from Tasiilaq, Greenland, maintained by the Danish Meteorological Institute (http://ocean.dmi.dk/tides/tides_grl.php). We then utilized T_TIDE, a tidal harmonic analysis toolbox (Pawlowicz, 2002), to estimate the amplitudes and phases of the principal lunar (M2) and solar (S2) semidiurnal tidal components. To compare calving episodes with tidal phase, we isolated calving episodes identified between two sequential time-lapse images – where calving must have occurred within the 3-hour time window represented between the images – and calculated the tidal phases associated with the calving time intervals.

OBSERVATIONS AND RESULTS

Figure S2 shows the distribution of calving episodes relative to both the high-low semidiurnal and spring-neap semimonthly tidal cycles. It is difficult to discern any meaningful pattern from the calving distribution with the semidiurnal tidal phase, possibly because the time between time-lapse image frames (3 hours) is roughly one-quarter of the total semidiurnal tidal cycle (Figure S2a). There is, however, a relationship between calving episode timing and spring-neap tidal phase (Figure S2b), with most nontabular calving occurring during the transition from spring to neap tide or near neap tide. Forty of the 52 nontabular calving episodes (77%) occurred over the half of the cycle defined by the range $2\pi/3$-$5\pi/3$ (120°-300°), where zero is defined as the neap to spring marker. Conversely, all five mixed calving episodes occurred within the 183.4° range between 24.3° and 207.7° – closer to spring tide.

Tidal cycles could influence calving at marine-terminating glaciers, but the spatial variability in basal coupling across Helheim Glacier's terminus may complicate this relationship. Further research is needed to understand the relationship between calving and tidal phase in various grounding states.

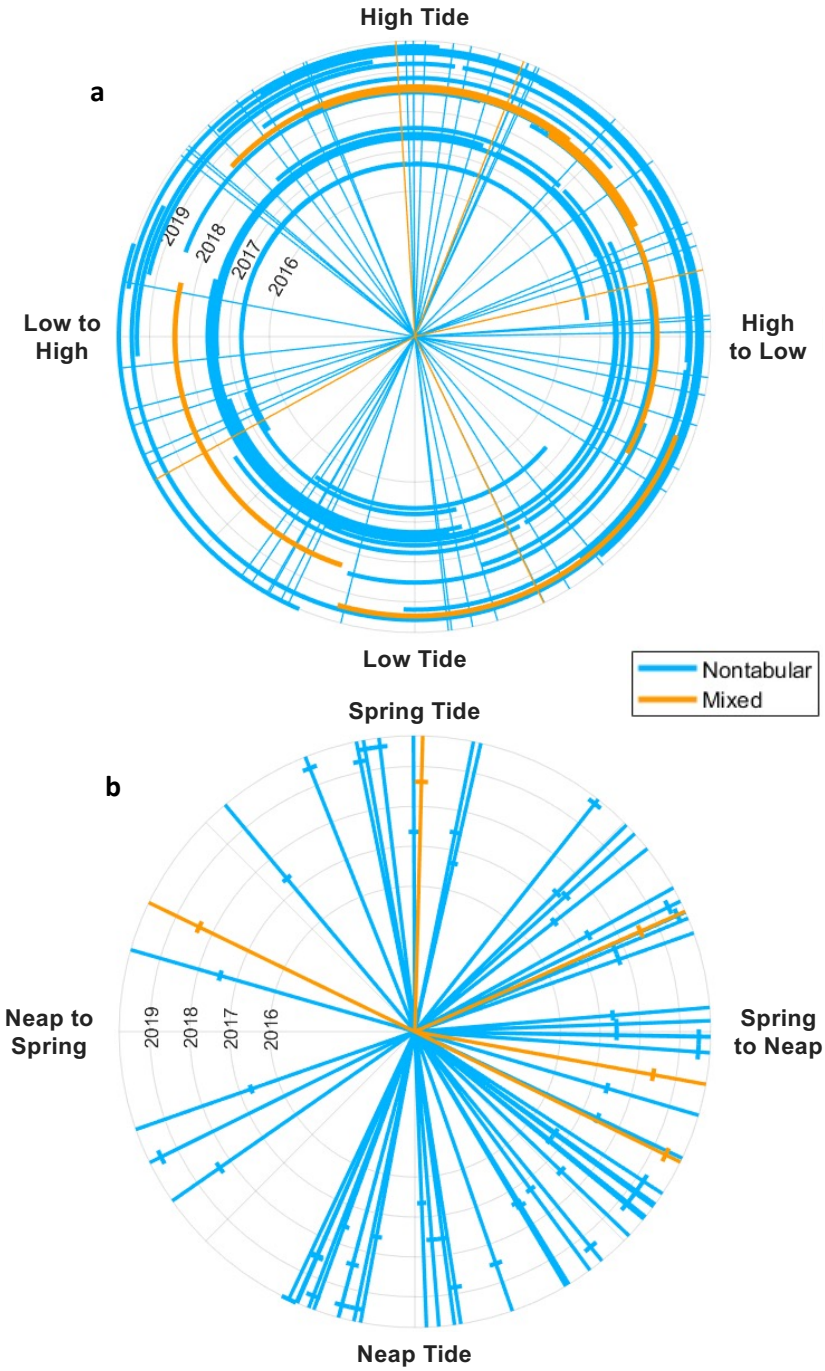

Figure S2: Distribution of calving episodes with tidal phase, from 2016 through 2019. The circular plots - oriented clockwise - represent tidal phase, both the (a) semidiurnal high-low tidal cycle and (b) semimonthly spring-neap tidal cycle. Teal and orange lines mark nontabular and mixed calving episodes, respectively. Because each calving episode could have occurred in a three-hour time interval (between two consecutive time-lapse images), the radial lines emanating from the center mark the tidal phase at the middle of the time interval (1.5 hours). The intersecting arc lines represent the range of tidal phases for the entire time interval (3 hours) and are plotted by calving date, with time along the radial axis.

REFERENCES

Erofeeva S and Egbert G (2020) Arc5km2018: Arctic Ocean Inverse Tide Model on a 5 kilometer grid, 2018. Arctic Data Center. doi:10.18739/A21R6N14K

Pawlowicz R, Beardsley B, and Lentz S (2002) "Classical Tidal Harmonic Analysis Including Error Estimates in MATLAB using T_TIDE", *Computers and Geosciences*. 28, 929-937.